Published in final edited form as:
Biomacromolecules. 2012 February 13; 13(2): 358–368. doi:10.1021/bm201372u.

Lubricated Biodegradable Polymer Networks for Regulating Nerve Cell Behavior and Fabricating Nerve Conduits with a Compositional Gradient

Lei Cai[†], **Jie Lu**[§], **Volney Sheen**[§], and **Shanfeng Wang**[†,‡,*]

[†]Department of Materials Science and Engineering, The University of Tennessee, Knoxville, TN 37996

[‡]Biosciences Division, Oak Ridge National Laboratory, Oak Ridge, TN 37831

[§]Department of Neurology, Beth Israel Deaconess Medical Center, Harvard Medical School, Boston, MA 02115

Abstract

We present a method of tuning surface chemistry and nerve cell behavior by photo-crosslinking methoxy poly(ethylene glycol) monoacrylate (mPEGA) with hydrophobic, semi-crystalline poly(ε-caprolactone) diacrylate (PCLDA), at various weight compositions of mPEGA (ϕ_m) from 2 to 30%. Improved surface wettability is achieved with corresponding decreases in friction, water contact angle, and capability of adsorbing proteins from cell culture media because of repulsive PEG chains tethered in the network. The responses of rat Schwann cell precursor line (SpL201), rat pheochromocytoma (PC12), and E14 mouse neural progenitor cells (NPCs) to the modified surfaces are evaluated. Non-monotonic or parabolic dependence of cell attachment, spreading, proliferation, and differentiation on ϕ_m is identified for these cell types with maximal values at ϕ_m of 5–7%. In addition, NPCs demonstrate enhanced neuronal differentiated lineages on the mPEGA/PCLDA network at ϕ_m of 5% with intermediate wettability and surface energy. This approach lays the foundation for fabricating heterogeneous nerve conduits with a compositional gradient along the wall thickness, which are able to promote nerve cell functions within the conduit while inhibiting cell attachment on the outer wall to prevent potential fibrous tissue formation following implantation.

Keywords

polyethylene glycol (PEG); poly(ε-caprolactone) diacrylate (PCLDA); surface wettability; nerve conduit; nerve cell behavior

Introduction

Injuries to the nervous systems are challenging medical problems that may lead to life-long disabilities.[1–4] Tissue engineering nerve guides made from biodegradable polymers have been extensively explored and offer novel therapeutic approaches, especially for peripheral nerve injuries.[1–6] For central nervous system (CNS) damage caused by trauma or disease

*Corresponding author. swang16@utk.edu; Tel: 865-974-7809; Fax: 865-974-4115.

Supporting Information Available: Storage modulus G', loss modulus G'', and viscosity η as functions of frequency for crosslinked mPEGA/PCLDA at 60 °C. Complete information about SpL201 and PC12 cell phenotype, attachment, and area as well as NPC phenotype and attachment on crosslinked mPEGA/PCLDA disks. This material is available free of charge via the Internet at http://pubs.acs.org.

(e.g. spinal cord injury), current interventions are still unsuccessful in achieving functional recovery despite numerous tissue engineering techniques.[3,4] Tubular scaffolds are needed in both scenarios for guiding and protecting axons.[1–7] An ideal nerve guide should facilitate neutropic and neutrophic communication between the proximal and distal ends of the nerve gap, block external inhibitory factors and undesired fibrous tissue that potentially elicits endoneurial scarring, and provide physical guidance and a permissive environment for fostering axonal regrowth.[1–7]

Injectable and photo-crosslinkable poly(ε-caprolactone) diacrylate (PCLDA; Figure 1) has great promise for diverse medical applications.[8] PCLDA can be synthesized using facile condensation between poly(ε-caprolactone) (PCL) diol and acryloyl chloride in the presence of potassium carbonate (K_2CO_3) which serves as a proton scavenger.[8,9] After photo-crosslinking, PCLDA networks have excellent cytocompatibility and convenient handling characteristics.[8] By varying the molecular weight of the PCL diol precursor, the crosslinking density and crystallinity of PCLDA network can be regulated simultaneously to obtain a wide range of mechanical properties.[8] Compared with PCL fumarate (PCLF) which has been used to fabricate nerve conduits for guiding axonal growth,[10,11] PCLDA has more reactive acrylate end-capping segments and can more efficiently form networks with better-defined crosslinking density. Previously we have used PCLDA to demonstrate the feasibility of fabricating three-dimensional (3D) porous scaffolds and nerve conduits with desired geometries for potential applications including peripheral nerve regeneration.[8] In contrast to their amorphous counterparts, semi-crystalline PCLDA networks with higher stiffness, mechanical strength, and toughness could better support attachment, spreading, and proliferation of mouse MC3T3-E1 cells and rat conditionally immortalized Schwann cell precursor line (SpL201) cells.[8] PCLDA have also been blended and photo-crosslinked with hydroxyapatite (HA) nanoparticles[12] and polypropylene fumarate (PPF)[13] to improve bulk and surface properties and to regulate cell behavior in diverse tissue engineering applications.

Despite many advantages, the hydrophobic nature of semi-crystalline PCLDA networks limits their performance as nerve conduit materials. One reason is that poor wettability prohibits body fluids and nutrients from diffusing efficiently into the conduit. In addition, lack of surface lubrication increases the friction and inflammatory reactions around a conduit after implantation.[14] Tethering hydrophilic chains such as poly(ethylene glycol) (PEG) is one widely used method to improve surface wettability while suppressing protein adsorption and cell attachment.[14–17] Recently we crosslinked low-molecular-weight methoxy PEG monoacrylate (mPEGA; Figure 1) with hydrophobic PPF and found the wettability could be greatly improved and the surface was lubricated while the modified networks were not water-swellable, which are all advantageous for clinical applications.[18] When the mPEGA composition (ϕ_m) was 5–7% and the tethered PEG chains were sparsely distributed on the surface of crosslinked PPF/mPEGA, MC3T3-E1 cell attachment, spreading, proliferation, and differentiation were enhanced.[18]

The objective of this study was to modify the bulk and surface characteristics of semi-crystalline PCLDA networks by incorporating 0–30% mPEGA through photo-crosslinking (Figure 1) and to understand the effect of tethered PEG chains on the behavior of both neuronal and glial cells. Surface characteristics of polymer substrates such as chemistry, topology, and stiffness are crucial in regulating cell fate.[4,19] Cell types used in this study include rat pheochromocytoma (PC12), rat SpL201 cells, and embryonic day 14 (E14) mouse neural progenitor cells (NPCs). Glial SpL201 cells can differentiate into early Schwann cell-like cells, and upregulate Oct-6 and myelin gene expression upon forskolin treatment, which is used to mimic axonal signals *in vitro*.[20] PC12 cells are neuronal-like cells that can respond to nerve growth factor (NGF) and grow neurites *in vitro* and are a

widely used model for studying cell signaling and neuronal communication.[21] NPCs, one kind of self-renewing and multi-potent neural stem cells with more limited capacities in growth and differentiation, can produce differentiated, functional progeny including neurons and glial phenotypes and are used in transplantation to repair injured or diseased CNS.[22]

Using these three nerve cell types for different aspects in evaluating the polymer networks prepared in this study for nerve tissue engineering applications, we have characterized cell attachment, spreading, proliferation, and differentiation on the polymer surfaces and correlated with surface properties including stiffness, friction, hydrophilicity, and the capability of adsorbing proteins from culture media. Based on non-monotonic dependence of cell behavior on the composition of crosslinked mPEGA/PCLDA, we have fabricated heterogeneous compositional-gradient nerve conduits that are able to meet the requirement of promoting nerve cell functions inside the tube while preventing cell attachment on the outer surface. This study provides a possible solution to the long-existing problem of inhibiting undesirable scar tissue formation on a nerve graft.[1–4,6]

Experimental Section

Synthesis and Crosslinking

All chemicals were purchased from Sigma-Aldrich (Milwaukee, WI) unless otherwise noted. mPEGA (M_n = 330 g mol^{-1}, M_w = 420 g mol^{-1}) and PCLDA (M_n = 3510 g mol^{-1}, M_w = 5150 g mol^{-1}) were synthesized by reacting methoxy polyethylene glycol (mPEG) and PCL diol (M_n = 3470 g mol^{-1}, M_w = 5200 g mol^{-1}) with acryloyl chloride in the presence of K_2CO_3, respectively.[8,18] mPEGA and PCLDA were dissolved in CH_2Cl_2 to form homogeneous mixtures at ϕ_m of 0, 2%, 5%, 10%, 20%, and 30%. Polymer solutions mixed with photo-initiator phenyl bis(2,4,6-trimethyl benzoyl) phosphine oxide (BAPO, Irgacure 819™, Ciba Specialty Chemicals, Tarrytown, NY) were crosslinked with ultraviolet (UV) light (λ = 315–380 nm) from a Spectroline high-intensity long-wave UV lamp (SB-100P, Intensity: 4800 μw/cm^2) for 20 min. Except for the measurements of swelling ratio and gel fraction, crosslinked polymer samples (~8 × ~0.8 mm, diameter × thickness) were soaked in acetone to remove the sol fraction and completely dried in vacuum. Then these disks were compressed between two smooth glass plates at 60 °C when they were amorphous to minimize surface roughness induced by crystallization.

Characterization of Polymer Bulk Properties

The η_0 data of uncrosslinked mPEGA/PCLDA blends were measured from the Newtonian region at temperatures from 50 to 100 °C using a strain-controlled rheometer (RDS-2, Rheometric Scientific) donated by Patel Scientific in the frequency range of 0.1–100 rad/s. A parallel plate flow cell with a diameter of 25 mm and a gap of ~0.5 mm were used. FTIR spectra were obtained on a Perkin Elmer Spectrum Spotlight 300 spectrometer with a dedicated diamond Attenuated Total Reflectance (ATR) accessory. DSC measurements were performed on a Perkin Elmer Diamond differential scanning calorimeter in a nitrogen atmosphere. The same thermal history was kept for each sample by first heating from room temperature to 100 °C and then cooling to −80 °C at 10 °C/min. A subsequent heating run was performed from −80 to 100 °C at 10 °C/min. Using the methods reported by us 6, the swelling ratios of mPEGA/PCLDA networks were determined by immersing two crosslinked disks (~8 × ~1.0 mm, diameter × thickness) in PBS and CH_2Cl_2 separately, while the gel fractions were measured only in CH_2Cl_2. The rheological properties of crosslinked samples were performed at 37 and 60 °C with a small strain (γ = 1%) with an 8 mm diameter parallel plate flow cell and a gap of ~0.5 mm, depending on the thickness of polymer disk. The tensile properties of crosslinked mPEGA/PCLDA specimens were implemented at 37 °C on a dynamic mechanical thermal analyzer (DMTA-5, Rheometric

Scientific). Briefly, polymer strips (~30 × ~1.5 × ~0.3 mm, length × width × thickness) were pulled at a strain rate of 0.001 s^{-1}. At least five specimens for each sample were measured and averaged.

Characterization of Polymer Surface Properties

Frictional forces between a stainless steel plate and hydrated crosslinked mPEGA/PCLDA disks were measured using the same rheometer and the method reported previously.[18] Hydrophilicity of the disks was quantified by the water contact angle measurements using a Ramé-Hart NRC C. A. goniometer (model 100-00-230).[8] Protein adsorption on the disks was evaluated by immersing crosslinked mPEGA/PCLDA disks in the culture media for rat SpL201 cells for 4 h at 37 °C. A MicroBCA protein assay kit (Pierce, Rockford, IL) was used for quantification with albumin for constructing a standard curve.[8] Surface morphology of crosslinked mPEGA/PCLDA disks was characterized using AFM (Nanoscope III control system, Veeco Instruments, Santa Barbara, CA). Images were acquired in the tapping mode at room temperature with a scan size of 20 × 20 μm and a scan rate of 0.5 Hz. Surface topography was recorded simultaneously with a standard silicon tapping tip on the beam cantilever. Root mean square (rms) roughness (R_{rms}) was calculated and averaged from the height profiles of three AFM images.

In vitro SpL201 and PC12 Cell Attachment, Proliferation, and Differentiation

Rat SpL201 cells were cultured in a growth medium consisting of Dulbecco's modified eagle media (DMEM; Gibco, Grand Island, NY), 10% fetal bovine serum (FBS, Gibco), 1% penicillin/streptomycin (Gibco), and 10 ng mL^{-1} human recombinant EGF (Pepro Tech Inc., Rocky Hill, NJ). Rat PC12 cells were cultured in a growth medium containing F-12K media (Gibco), 15% horse serum, 5% FBS and 1% penicillin/streptomycin in an incubator with 5% CO_2 and 95% relative humidity at 37 °C. SpL201 and PC12 cells were seeded onto 70% alcohol-sterilized disks of crosslinked mPEGA/PCLDA at a density of ~15,000 cells per cm^2 for 4 h, 1, 4, and 7 days. A colorimetric cell metabolic assay (CellTiter 96 Aqueous One Solution, Promega, Madison, WI) was performed on three parallel samples from one group at each time point. Using a standard curve, the number of viable cells was correlated to the UV absorbance at 490 nm measured on a microplate reader. For differentiation, SpL201 cells were treated with differentiation medium containing DMEM, 10% FBS, 1% penicillin/streptomycin without EGF, but with 20 μM forskolin for 7 days. PC12 neurites were induced in a growth medium supplemented with 50 ng mL^{-1} NGF for 7 days. Cells were fixed in 4% paraformaldehyde (PFA) solution for 10 min and blocked with PBS containing 0.3% Triton X-100 and 1% bovine serum albumin (BSA) at room temperature for 30 min at room temperature. Fluorescent images were taken on both cells and PC12 neurites stained using RP (Cytoskeleton Inc., Denver, CO) on an Axiovert 25 light microscope (Carl Zeiss, Germany). Differentiated SpL201 cells were stained with primary antibody of mouse monoclonal anti-oligodendrocyte marker O4 antibody (1:1000; R&D Systems, Minneapolis, MN) at 37 °C for 1 h and then at 4 °C overnight. Cells were washed using PBS containing 1% BSA for three times, and stained with secondary antibody of goat anti-mouse IgM-FITC (1:100) at 37 °C in the dark for 2 h. After washing with PBS for three times, cells were counter-stained with 4',6-diamidino-2-phenylindole (DAPI) at room temperature for photographing. SpL201 cell area and PC12 cell neurites were analyzed and averaged from at least 100 cells.

In vitro NPC Cell Attachment, Proliferation, and Differentiation

E14 mouse NPCs were cultured in serum-free growth media containing DMEM/F12 media (Invitrogen) with 2% StemPro neural supplement (Invitrogen), 20 ng mL^{-1} basic fibroblastic growth factor (bFGF; Invitrogen), 20 ng mL^{-1} epidermal growth factor (EGF recombinant human, Invitrogen), 1% GlutaMAX (Invitrogen), and 1% penicillin/streptomycin. NPC cell

attachment and proliferation were performed and analyzed using the same procedure for SpL201 cells mentioned earlier. For NPC differentiation, the growth media were removed after cells attached onto the polymer disks and replaced with the differentiation media containing DMEM/F12 media, 1% FBS, 1 μM all-*trans*-retinoic acid, and 1% GlutaMAX. NPCs were cultured in the differentiation media for additional 7 days. After fixation and blocking, cells were incubated with a diluted primary antibody, mouse monoclonal anti-β-tubulin III (1:500) for neurons or mouse monoclonal anti-GFAP (1:500) for astrocytes, at 37 °C for 1 h and then at 4 °C overnight. After being washed in PBS that contains 1% BSA for three times, cells were stained with a secondary antibody of goat anti-mouse IgG-FITC (1:100) at 37 °C in the dark for 2 h. Finally cell nuclei were counter-stained using DAPI for photographing. Differentiation in terms of positive antibody expression was quantified by counting the number of cells in each image that expressed the marker and dividing it by the total number of cells identified by DAPI staining. At least 10 images were analyzed and averaged.

Nerve Conduit Fabrication

Using a mold composed of a glass tube, a stainless steel wire, and two Teflon end-caps,[10] homogeneous nerve conduits were fabricated by transferring and photo-crosslinking mPEGA/PCLDA precursor solutions (ϕ_m = 5%) in the mold. Heterogeneous nerve conduits were fabricated by dipping the steel wire with mPEGA/PCLDA precursor solutions (ϕ_m = 5%) and placed in the center of the mold. Then mPEGA/PCLDA precursor solution (ϕ_m = 30%) was injected into the mold. The filled mold was rolled to allow two solutions to diffuse extensively prior to photo-crosslinking. All the conduits were crosslinked, purified, and sterilized in the same fashion mentioned previously. SpL201 cells was seeded by immersing the polymer tubes in a growth medium with floating cells and cultured for 1 day before fixation. The PEG compositions of the compositional-gradient nerve tube at different positions along the wall thickness were characterized using FTIR. The cross-section of the tube was cut and placed on the sample stage whose movement could be precisely controlled. FTIR spectra were obtained from a single pixel of 25 × 25 μm at positions of 0, 20%, 40%, 60%, and 100% of the thickness from the inner to the outer wall.

Statistical Analysis

All statistical computations were performed by analysis of variance (ANOVA) followed by Tukey post-test as needed. The values were considered significantly different if the *p*-value was less than 0.05.

Results and Discussion

Bulk Characteristics

Homogeneous mixtures of mPEGA/PCLDA with different ϕ_m were characterized in terms of zero-shear viscosity (η_0) at temperatures from 50 to 100 °C (Figure 2a). This measurement range was above the melting temperature (T_m) of semi-crystalline PCLDA, 49.1 °C.[8] Blending mPEGA short chains into PCLDA could significantly decrease η_0. At 50 °C, η_0 was 0.63 Pa.s for PCLDA and this value decreased progressively to 0.22 Pa.s for mPEGA/PCLDA (ϕ_m = 30%). η_0 further decreased with increasing temperature. For mPEGA/PCLDA (ϕ_m = 30%) at 100 °C, it was only 0.06 Pa.s. Lower η_0 achieved by adding mPEGA could facilitate flow of PCLDA and improve its injectability or processability in stereolithographic fabrication of conduits or scaffolds.

The chemical structures of crosslinked mPEGA/PCLDA were characterized using FTIR spectra (Figure 2b). The absorption peaks assigned for crosslinked PCLDA were dominant in the spectra. For example, prominent peaks at 1740 and 2950 cm^{-1} were found for ester

carbonyl and methylene groups, respectively. The peak for vinyl groups at 1635 cm^{-1} observed in the spectrum of mPEGA was not evident for the crosslinked samples, suggesting that the carbon-carbon double bonds were largely consumed through efficient crosslinking.

The gel fraction of crosslinked mPEGA/PCLDA varied gradually from ~80% to ~70% when ϕ_m increased from 0 to 30% (inset of Figure 2c). The values were sufficiently high for the networks to maintain integrity after removal of the sol fraction using a good solvent, CH_2Cl_2. The gel fraction of the polymer network in water was close to 100%, indicating that there was no discernible loss of PEG chains in water, similar to mPEGA/PPF networks.[18] Because mPEGA could polymerize by itself, crosslinked mPEGA/PCLDA with higher ϕ_m had lower crosslinking densities, as evidenced by the higher swelling ratios in CH_2Cl_2 (Figure 2c). In contrast, only very slight swelling (< 10%) was found in water even at ϕ_m of 30%, owing to the hydrophilic nature of grafted PEG chains. The minimal amount of water trapped in the networks prevents any distortion in the shape and dimension of the scaffold during fabrication and surgical implantation.

The thermal properties of crosslinked mPEGA/PCLDA characterized using the differential scanning calorimetric (DSC) curves (Figure 2d) are listed in Table 1. All the samples were semi-crystalline at 37 °C and the crystallinity decreased after incorporation of short, amorphous PEG chains. Because of this impairment to the crystalline domains and crystallite thickness, T_m also decreased slightly from 41.2 °C for crosslinked PCLDA to 37.6 °C for crosslinked mPEGA/PCLDA (ϕ_m = 30%). Meanwhile, a weak increase from −60.9 to −57.4 °C was found in the glass transition temperature (T_g) and it can be attributed to less chain segmental constraints from crystalline domains and crosslinks. A more drastic decrease of 11.1 °C was found for the crystallization temperature (T_c) determined from the cooling curve.

The rheological properties of mPEGA/PCLDA networks were measured at 37 and 60 °C as functions of frequency in the range of 0.1–100 rad s^{-1} to show the effects of both crystallinity and crosslinking density (Figures 2e and S1). Rubbery behavior was demonstrated for all the samples as the storage modulus G' had no frequency dependence and it was constantly higher than the loss modulus G''. Shear thinning behavior for viscosity (η) was observed for all the networks. Shear modulus G was the average value of G' in the tested frequency range. By increasing ϕ_m, G (Table 1) and η (Figure 2e) at body temperature were lower for mPEGA/PCLDA networks because of lower crystallinities and crosslinking densities. At 60 °C, all the networks were amorphous and there only existed the pure effect of crosslinking density, which is inversely proportional to the average molecular weight (M_c) between two neighboring crosslinks.[11,13] The mechanical properties of mPEGA/PCLDA networks were determined at 37 °C, a temperature at which both effects of crystallinity and crosslinking density were present. Representative tensile stress-strain curves are shown in Figure 2f and the results such as tensile moduli (E), tensile stress (ε_b) and strain (ε_b) at break are listed in Table 1. Because both crystallinity and crosslinking density were reduced by introducing PEG short dangling chains, E and σ_b decreased while ε_b increased with increasing ϕ_m by factors of 10.5, 2.6, and 2.9, respectively. The monotonic trend was consistent with previously reported mPEGA/PPF networks, where grafted PEG significantly decreased the crosslinking density and stiffness of the PPF network.[18]

Surface Characteristics

The surface characteristics of PCLDA network were drastically modified by the tethered PEG chains. For estimating PEG chain coverage on the surface of PCLDA network,[18] we used the Kuhn length b of 0.7 nm for both PEG[24] and PCL[25] and the number of repeating units, N, from the molecular weight to calculate the mean-square radius of gyration R_g^2 for

tethered polymer chains using eq. 1 below.[26] The result for mPEGA ($R^2_{g,m}$) was 0.9 nm^2 and for PCLDA ($R^2_{g,PCLDA}$) was 5.0 nm^2. The molar compositions of mPEGA (Φ_m) in mPEGA/PCLDA blends with ϕ_m of 2%, 5%, 7%, 10%, 20%, and 30% were 17%, 36%, 44%, 54%, 72%, and 82%, respectively. Accordingly, the approximate coverage (C) of grafted PEG chains on the surface of crosslinked mPEGA/PCLDA could be 3.6%, 9.2%, 12%, 17%, 31%, and 45% estimated using eq. 2, indicating that the PEG pendant chains with a wide range of densities were tethered on the PCLDA network surfaces.

$$R_g^2 = \frac{r_0^2}{6} = \frac{(N^{3/5}b)^2}{6} \quad (1)$$

$$C = \frac{R^2_{g,m} \cdot \Phi_m}{R^2_{g,m} \cdot \Phi_m + R^2_{g,PCLDA} \cdot (1 - \Phi_m)} \quad (2)$$

Lubricated surfaces are desirable for many tissue-contacting medical devices such as catheters, endoscopes, and contact lenses, because a slippery surface with a low friction could facilitate easy insertion and removal from a patient.[27] As mentioned earlier, polymer nerve conduits with lubricated surfaces can allow for better movement and adjustment in implantation. PEG-grafted surfaces have been widely used to create surfaces with lower frictions.[15,28] The frictional behavior of hydrated crosslinked mPEGA/PCLDA disks measured using rheometry[28] conformed to Amonton's law $\mathcal{F} = \mu W$, a linear relationship between the frictional force $\mathcal{F}$ and the normal force W, as demonstrated in the inset of Figure 3a. The frictional coefficient μ calculated from the slope of fitted straight lines decreased continuously by 7-fold from 0.37 ± 0.02 for crosslinked PCLDA to 0.05 ± 0.01 for mPEGA/PCLDA (ϕ_m = 30%). Similar to mPEGA/PPF networks, the sharp decrease in μ suggested that PEG chains could appear on the surface of PCLDA network as well as in the bulk and consequently modified interfacial interactions, leading to hydrodynamic lubrication. Unlike HA nanoparticles that could be buried underneath the crystalline PCLDA network surface,[12] tethered PEG chains showed a great advantage as to improve surface properties of crystalline polymer networks. The remarkable lubricating effect (μ ≤ 0.03) was also reported in PEG-modified polydimethylsiloxane when ϕ_m was higher than 10%.[15]

The existence of PEG chains covalently tethered on the network surface can also be confirmed by characterizing surface hydrophilicity using the water contact angle and the capability of protein adsorption from cell culture media. As shown in Figure 3b, the water contact angle decreased monotonically on crosslinked mPEGA/PCLDA blends with more grafted PEG chains. The improved hydrophilicity by adding mPEGA was originated from the hydrophilic nature of PEG chains tethered in the network that could also appear on the surface. The ability of adsorbing serum proteins also decreased progressively with increasing ϕ_m because of the well-known repulsive effect of PEG tethered chains.[14,16]

Surface topography demonstrated by the atomic force microscopy (AFM) images in Figure 3c was similar among PCLDA networks grafted with different mPEGA amounts and no significant difference was found for R_{rms} (Table 1). Because the purified polymer disks were compressed prior to use, the surfaces of mPEGA/PCLDA networks were much smoother (~15 nm) than those of semi-crystalline crosslinked PCLDA (260 nm) and PPF/PCLDA disks (> 70 nm) reported previously.[8,13] The impact of surface roughness on nerve cell behavior can be neglected in later discussion.

In vitro SpL201 Cell Behavior

Surface characteristics of polymer substrates are crucial in determining the behavior of cells seeded on them.[4,19] As discussed previously, monotonic changes in mechanical properties, friction, hydrophilicity, and protein adsorption from culture media were observed for mPEGA/PCLDA networks. Similar to PCLDA networks, no detectable degradation was found for mPEGA/PCLDA networks in phosphate buffered saline (PBS) at 37 °C in two weeks.

Cell densities in the fluorescent images of SpL201 cells stained using rhodamine-phalloidin (RP) at days 1, 4, and 7 (Figures 4a and S2a) were consistent with the cell numbers (Figure 4b) measured using fluorescence-based assay. As the initial step to regulate cell motility, growth, and other functions, cell adhesion is crucial in sensing polymer surfaces. SpL201 cell adhesion at 4 h post-seeding quantified by the cell number (Figure 4b) and normalized cell attachment (Figure S2b) showed a non-monotonic or parabolic trend of first increasing from crosslinked PCLDA to crosslinked mPEGA/PCLDA (ϕ_m = 5–7%). Cell number and normalized cell attachment subsequently decreased sharply to crosslinked mPEGA/PCLDA (ϕ_m = 30%). These results indicated that SpL201 cell attachment was promoted on substrates with sparsely distributed PEG chains, whereas it was inhibited when PEG chains were dense. Similar to the enhanced cell attachment, the average cell spreading area at day 1 (Figure S2c) also had a maximum on crosslinked mPEGA/PCLDA ϕ_m = 5%) and cell proliferation exhibited parabolic dependence on ϕ_m and maximized at ϕ_m of 5–7% (Figure 4b). The proliferation index of SpL201 cells, calculated by dividing the cell number at day 7 by the attached cell number at 4 h, increased from 4.09 ± 0.13 on crosslinked PCLDA to 4.79 ± 0.43 at ϕ_m of 7%, and then decreased to 3.64 ± 0.49 at ϕ_m of 20%.

A previous study found that surface energy of polymer substrates could influence Schwann cell attachment and proliferation in a non-monotonic manner, with the highest cell density on poly(ethyl acrylate-*co*-hydroxyethyl acrylate) copolymers with intermediate surface energies.[26] Integrin binding between cell membrane receptors and adsorbed proteins on the surface mediates cell adhesion.[14,19] Integrin binding is sensitive to quantity, spatial arrangement, and orientation of adhesion motifs in the extracellular matrix (ECM) proteins, the amount and conformation of which depend on both surface energy and entropy.[14,19,29] Generally hydrophobic surfaces will induce adsorption of non-adhesive proteins and denaturing of adhesive proteins while hydrophilic surfaces will result in low protein binding.[14,19] Therefore, the balance of both driving forces on surface with intermediate energies for adsorption can lead to a maximum value for cell adhesion.

The differentiation potential of SpL201 cells after forskolin treatment was quantified using O4 antibody (Figure 4a,c), an indicator to distinguish early Schwann cells from undifferentiated SpL201 cells.[20] Strikingly, the differentiated cell area measured from the cells stained with O4 antibody was largest on crosslinked mPEGA/PCLDA ϕ_m = 5%), suggesting the potential of the PCLDA network, modified using a small amount of tethered PEG chains, in upregulating SpL201 cell differentiation to early Schwann cells, which were mitotically active and could differentiate into fully myelinating Schwann cells when interacting with axons *in vitro*.[20]

In vitro PC12 Cell Behavior

In contrast to the monotonic dependence on composition for all the mPEGA/PCLDA network material properties, non-monotonic or parabolic trends were appreciated not only for the glial-natured SpL201 cells, but also for attachment, proliferation, and differentiation of neuronal-natured PC12 cells. The fluorescent images of RP-stained PC12 cells on crosslinked mPEGA/PCLDA disks at days 1, 4, and 7 (Figures 5a and S3a) demonstrate

both proliferation and differentiation levels. Though PC12 cell attachment did not show significant differences among ϕ_m of 0–7% (Figure S3b), they could spread out over a larger area and proliferate faster on the substrates with ϕ_m of 5–7%, compared with other compositions (Figures 5b and S3c). The proliferation index of PC12 cells increased greatly from 4.72 ± 0.18 on crosslinked PCLDA to 6.45 ± 0.83 at ϕ_m of 7%, and then decreased dramatically to 1.58 ± 0.81 at ϕ_m of 30%. Upon NGF treatment, the number of neurites per PC12 cell was significantly higher on the substrates with ϕ_m of 5–7% than that on crosslinked PCLDA (Figure 5a,c). When ϕ_m was higher than 20%, no neurite extension could be observed. The extent of differentiation characterized by the percentage of cells bearing neurites was promoted by the tethered PEG chains on the surfaces with ϕ_m of 5–7% and the neurite length also exhibited the same trend. Neurites had average lengths of 67 ± 27 and 65 ± 15 μm on crosslinked mPEGA/PCLDA disks with ϕ_m of 5% and 7%, respectively. They were significantly longer than the lengths of 49 ± 14 and 35 ± 13 μm for the neurites on crosslinked PCLDA and crosslinked mPEGA/PCLDA (ϕ_m = 20%), respectively.

In a previous study on a wettability-gradient polyethylene (PE) surface, neurite formation of PC12 cells was enhanced in regions with moderate hydrophilicity than those in more hydrophobic or more hydrophilic regions.[30] Distribution of surface energy could trigger mechanisms for driving PC12 cells to differentiate and initiate neuritogenesis through cell-material interactions.[31] Integration of signaling pathways initiated by integrins and protein tyrosine kinases (Pyk) on the cell membrane is one essential factor for NGF-mediated PC12 neurite formation.[32] The focal-adhesion kinase (FAK) family is subsequently activated to promote outgrowth of neurites in PC12 cells.[32] Therefore, Pyk2 and FAK work collectively to integrate signals proximal to integrins and NGF receptors which are sensitive to surface energy. Activation of Pyk2/FAK by integrins and growth factors is crucial for generating efficient signal cascades via pathways including paxillin that lead to the regulation of neurite outgrowth.[29] Other protein activities such as Rac1, RhoA and Cdc42 GTPases, and vinculin could be triggered on surfaces with intermediate surface energy.[31] These proteins modulate filopodia and lamellipodia assembly and disassembly in response to polymer surfaces and NGF, as well as the formation and stabilization of focal adhesions.[31] Variation of ion channels such as intracellular Ca^{2+} in PC12 cells induced by surface energy can be another factor. Filopodia extended by PC12 cells can induce elevation of intracellular Ca^{2+} that is propagated back to the growth cone, a process that is involved in neurite outgrowth,[33] though the exact mechanism for signal transduction of surface energy to cell nuclei is still an open question.

In vitro NPC Behavior

The potential of this series of mPEGA/PCLDA networks for CNS recovery was evaluated using NPCs in serum-free media, where the effect of ECM protein adsorption from serum could be eliminated. Crosslinked mPEGA/PCLDA (ϕ_m = 5%) demonstrated significantly better NPC attachment and proliferation than crosslinked PCLDA and mPEGA/PCLDA networks with ϕ_m greater than 10% (Figures 6a,b and S4). The proliferation index of NPCs first increased from 2.31 ± 0.30 on crosslinked PCLDA to 2.55 ± 0.19 at ϕ_m of 5%, and then decreased to 1.36 ± 0.11 at ϕ_m of 10%. This result suggested NPC proliferation was more likely to be inhibited on hydrophilic surfaces than SpL201 and PC12 cell proliferation. The non-monotonic trend with surface wettability was illustrated previously by clonal growth of human pluripotent stem cells which exhibited best clonal formation on polymer surfaces with water contact angles between 60° and 80°.[34] The proliferation rate of human bone marrow stem cells was also highest in the region with water contact angles between 48° and 97° on a gradient PE surface.[35]

The differentiation media we used could direct NPCs into two major neural lineages: neurons and astrocytes. No significant difference was observed in astrocytes on crosslinked

mPEGA/PCLDA disks with ϕ_m less than 10%, as demonstrated by the percentage of cells positive to glial fibrillary acidic protein (GFAP) antibody (Figure 6c). In contrast, more neurons expressing β-tubulin-III were found on crosslinked mPEGA/PCLDA with ϕ_m of 5–10% (Figure 6c), indicating their differentiation potential can be enhanced by optimizing the surface chemistry. Less support for both lineages was observed when ϕ_m was higher than 10%. Though there lacks a direct mechanism to elucidate the lineage commitment of NPCs on surface wettability, tethered small molecules with functional groups were reported to actively modify the stem cell niche.[36] Enhanced neuronal differentiation on the modified surfaces may be beneficial for directing particular cell differentiated lineage via a local gradient in surface wettability, as one alternative way yet to be explored in stem cells other than well-investigated substrate properties such as surface stiffness.[37]

Besides the effect of tethered PEG chains, surface stiffness could also be involved in regulating nerve cell behavior.[4,19,38] Unlike neuronal cells that attach and proliferate better on softer substrates with elasticity from 0.1 kPa to 1 MPa,[14,37,38] SpL201 cells were found to prefer stiffer polymer substrates in the studied range of *E* from 1 MPa to 1 GPa.[8,10,11,13] The effect of tethered PEG chains was so dominant that SpL201 cell attachment and proliferation did not decrease when in the *E* of crosslinked mPEGA/PCLDA decreased from 83.0 to 46.1 MPa in the ϕ_m range of 0–5%, and those of neuronal PC12 cells and NPCs did not increase when the *E* decreased from 46.1 to 8.9 MPa in the ϕ_m range of 5–30%. Note that the effect of surface stiffness on the cell behavior might be less prominent when the substrates have *E* higher than or lower than a critical value. How different surface characteristics, especially surface chemistry and stiffness, work collectively in regulating cell behavior still requires further investigation.

Nerve Conduits with Compositional Gradient

Inhibiting undesired tissue formation on the outer wall of a nerve conduit while promoting axonal growth inside is important because invasion of other cell types during implantation will be detrimental to axon survival.[1,2,5,6] Based on the finding of distinct nerve cell responses to two-dimensional (2D) substrates of crosslinked mPEGA/PCLDA with different ϕ_m, we have further designed 3D heterogeneous nerve conduits (Figure 7a) with a compositional gradient along the wall thickness, thereby addressing the feasibility of promoting nerve cell functions inside while prohibiting cell attachment outside. The composition of PEG at different positions along the conduit wall was characterized using FTIR spectra in Figure 7b. The ratio of the absorption of asymmetric C-O-C band at 1106 cm^{-1} (A_{1106}) from PEG chains to the C=O band at 1720 cm^{-1} (A_{1720}), indicating the composition of PEG, increased gradually from the inner wall to the outer wall (Figure 7c). Using both homogeneous and heterogeneous nerve conduits, we have examined SpL201 cell attachment and phenotype at day 1 and the results are shown in Figure 7a. After being immersed in SpL201 cell culture media containing dissociated cells, the nerve conduits provided attachment sites along both the inner and outer walls. SpL201 cells attached well on the inner walls of both homogeneous and heterogeneous conduits and the outer wall of the homogeneous conduit because they all contained 5% mPEGA. In clear contrast, SpL201 cells could not survive on the outer wall of the heterogeneous tube, which was composed of 30% mPEGA. The results confirmed the concept of fabricating nerve conduits with a compositional gradient to prevent initial cell attachment and may suggest a potential method of suppressing fibrous tissue formation outside in implantation, considering densely grafted PEG chains could strongly repel proteins and cells. A recent study using 2-methacryloyloxyethyl phosphorylcholine polymer coating on silastic elastomers indeed indicated that the inhibition of fibroblast cell adhesion and growth has a negative impact on *in vivo* fibrous tissue formation.[39] It is worthwhile to further examine such correlation using the present PEG-grafted polymer networks.

PEG chains were tethered not only on the surface but also inside the bulk of the polymer networks. The present method has advantages over other surface modification techniques such as self-assembled monolayers or surface-initiated polymerization because mPEGA/PCLDA networks were able to maintain the presence of PEG pendant chains even after degradation. By incorporating mPEGA short chains into PCLDA, the injectability and processability could be improved as the viscosity was reduced. The shape of the nerve conduits remained unaltered in water with negligible swelling because of the hydrophobic nature of the major component of crosslinked PCLDA. These nerve conduits also had sufficient mechanical strength and flexibility for holding sutures in the repair of large nerve gaps, similar to previously reported crosslinked PCLF nerve conduits implanted in rats.[10] In addition, lubricated surfaces with improved wettability by having a small amount of PEG pendant chains can facilitate implantation of nerve conduits and cause less wear between medical devices and surrounding tissues. We will evaluate the *in vivo* performance of these nerve conduits with multiple components and a compositional gradient and further explore to understand the underlying mechanisms of distinct nerve cell behaviors on these materials with tunable surface characteristics.

Conclusions

mPEGA end-capped with one double bond has been photo-crosslinked with semi-crystalline PCLDA to modify the bulk and surface properties of crosslinked PCLDA. Surface characteristics such as frictional coefficient, hydrophilicity, and protein adsorption were greatly altered by adding mPEGA. Improved surface lubrication, hydrophilicity, and reduced protein adsorption played collective roles in regulating rat SpL201 and PC12 cell attachment, spreading, proliferation, and differentiation. The proliferation rate of both cell types was first promoted by moderate hydrophilicity at ϕ_m of 5–7% and then was inhibited because of strong protein resistance from densely grafted PEG chains. The same non-monotonous trend was found in SpL201 differentiation upon foskolin treatment and PC12 neurite extension which was promoted by intermediate surface energy and wettability from sparsely distributed PEG chains. NPCs also demonstrated a significantly higher proliferation rate on the substrates with ϕ_m of 5% than on crosslinked PCLDA and surfaces tethered with more PEG chains. Neuronal lineages were favored on the substrates with low ϕ_m. Based on the parabolic dependence of cell behavior on the network composition, we have successfully prepared crosslinked mPEGA/PCLDA nerve conduits with a compositional gradient along the wall thickness. These heterogeneous nerve conduits can promote regenerative functions of nerve cells and foster axonal growth inside while inhibiting cell attachment in exterior during nerve regeneration.

Supplementary Material

Refer to Web version on PubMed Central for supplementary material.

Acknowledgments

This work was supported by the start-up fund of the University of Tennessee and National Science Foundation (DMR-11-06142) (to SW). We thank Xiaoming Jiang and Dr. Bin Zhao in the Department of Chemistry for the help with contact angle measurements, and Dr. Anthony J. Windebank and Jarred Nesbitt at Mayo Clinic for supplying rat SpL201 cells.

References

1. Schmidt CE, Leach JB. Annu. Rev. Biomed. Eng. 2003; 5:293. [PubMed: 14527315]
2. Chiono V, Tonda-Turo C, Ciardelli G. Int. Rev. Neurobiol. 2009; 87:173. [PubMed: 19682638]

3. Madigan NN, McMahon S, O'Brien T, Yaszemski MJ, Windebank AJ. Respir. Physiol. Neurobiol. 2009; 169:183. [PubMed: 19737633]
4. Norman LL, Stroka K, Espinoza HA. Tissue Eng. Part B. 2009; 15:291.
5. Wang S, Cai L. Int. J. Polym. Sci. 2010
6. Daly W, Yao L, Zeugolis D, Windebank A, Pandit A. J. R. Soc. Interface. 2011
7. Zhang N, Yan H, Wen X. Brain Res. Rev. 2005; 49:48. [PubMed: 15960986]
8. Cai L, Wang S. Polymer. 2010; 51:164.
9. Cai L, Wang S. Biomacromolecules. 2010; 11:304. [PubMed: 20000349]
10. Wang S, Yaszemski MJ, Knight AM, Gruetzmacher JA, Windebank AJ, Lu L. Acta Biomater. 2009; 5:1531. [PubMed: 19171506]
11. Wang S, Kempen DH, Simha NK, Lewis JL, Windebank AJ, Yaszemski MJ, Lu L. Biomacromolecules. 2008; 9:1229. [PubMed: 18307311]
12. Cai L, Wang S. Acta Biomater. 2011; 7:2185. [PubMed: 21284960]
13. Cai L, Wang S. Biomaterials. 2010; 31:7423. [PubMed: 20663551]
14. Roach P, Parker T, Gadegaard N, Alexander MR. Surf. Sci. Rep. 2010; 65:145.
15. Chawla K, Lee S, Lee BP, Dalsin JL, Messersmith PB, Spencer ND. J. Biomed. Mater. Res. 2009; 90A:742.
16. Lee JH, Lee HB, Andrade JD. Prog. Polym. Sci. 1995; 20:1043.
17. Lin L, Wang Y, Huang XD, Xu ZK, Yao K. Appl. Surf. Sci. 2010; 256:7354.
18. Cai L, Wang S. Biomaterials. 2010; 31:4457. [PubMed: 20202682]
19. a Saltzman, WM.; Kyriakides, TR. Principles of tissue engineering. 3rd ed. Lanza, R.; Langer, R.; Vacanti, J., editors. Elsevier Academic Press; San Diego, CA: 2007. p. 279-296.b Harbers, GM.; Grainger, DW. Introduction to biomaterials. Guelcher, SA.; Hollinger, JO., editors. Boca Raton, FL: Boca Raton: CRC Press; 2005. p. 15-45.
20. Lobsiger CS, Smith PM, Buchstaller J, Schweitzer B, Franklin RJ, Suter U, Taylor V. Glia. 2001; 36:31. [PubMed: 11571782]
21. Vaudry D, Stork PJS, Lazarovici P, Eiden LE. Science. 2002; 296:1648. [PubMed: 12040181]
22. a Gage FH. Science. 2000; 287:1433. [PubMed: 10688783] b Temple S. Nature. 2001; 414:112. [PubMed: 11689956]
23. Kavanagh GM, Ross-Murphy SB. Prog. Polym. Sci. 1998; 23:533.
24. Schultz KM, Baldwin AD, Kiick KL, Furst EM. Macromolecules. 2009; 42:5310. [PubMed: 21494422]
25. Herrera D, Zamora J, Bello A, Grimau M, Laredo E, Muller AJ, Lodge TP. Macromolecules. 2005; 38:5109.
26. a Halperin A, Tirrell M, Lodge TP. Adv. Polym. Sci. 1992; 100:31.b Zhao B, Brittain WJ. Prog. Polym. Sci. 2000; 25:677.
27. Ikada, Y.; Uyama, Y. Lubricating polymer surfaces. Technomic; Lancaster, PA, USA: 1993. p. 55-71.
28. a Gong JP, Kagata G, Osada Y. J. Phys. Chem. B. 1999; 103:6007.b Gong JP, Osada Y. Prog. Polym. Sci. 2002; 27:3.
29. Soria JM, Ramos CM, Bahamonde O, Cruz DMG, Sanchez MS, Esparza MAG, Casas C, Guzman M, Navarro X, Ribelles JLG, Verdugo JMG, Pradas MM, Barcia JA. J. Biomed. Mater. Res. 2007; 83A:463.
30. Lee SJ, Khang G, Lee YM, Lee HB. J. Colloid Interface Sci. 2003; 259:228. [PubMed: 16256501]
31. Lamour G, Journiac N, Souès S, Bonneau S, Nassoy P, Hamraoui A. Colloid. Surf. B. 2009; 72:208.
32. Ivankovic-Dikic I, Grönroos E, Blaukat A, Barth B, Dikic I. Nature Cell Biol. 2000; 2:574. [PubMed: 10980697]
33. Gomez TM, Robles E, Poo M, Spitzer NC. Science. 2001; 291:1983. [PubMed: 11239161]
34. Mei Y, Saha K, Bogatyrev SR, Yang J, Hook AL, Kalcioglu ZI, Cho S, Mitalipova M, Pyzocha N, Rojas F, Van Vliet KJ, Davies MC, Alexander MR, Langer R, Jaenisch R, Anderson DG. Nature Mater. 2010; 9:768. [PubMed: 20729850]

35. Shin YN, Kim BS, Ahn HH, Lee JH, Kim KS, Lee JY, Kim MS, Khang G, Lee HB. Appl. Surf. Sci. 2008; 255:293.
36. Benoit DSW, Schwartz MP, Durney AR, Anseth KS. Nature Mater. 2008; 7:816. [PubMed: 18724374]
37. Saha K, Keung AJ, Irwin EF, Li Y, Little L, Schaffer DV, Healy KE. Biophys. J. 2008; 95:4426. [PubMed: 18658232]
38. Discher DE, Janmey P, Wang YL. Science. 2005; 310:1139. [PubMed: 16293750]
39. Zhang Y, Kanetaka H, Sano Y, Kano M, Kudo T, Shimizu Y. Dent. Mater. J. 2010; 29:518. [PubMed: 20827031]

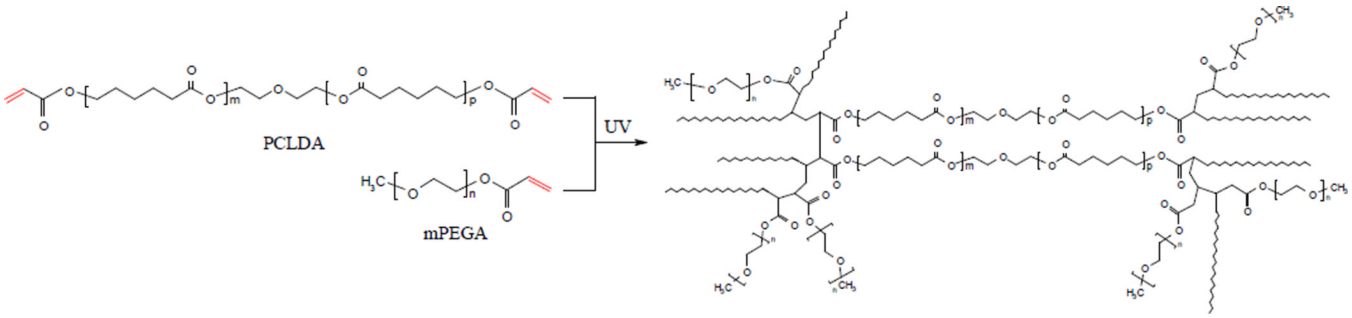

Figure 1.
Photo-crosslinking of mPEGA/PCLDA.

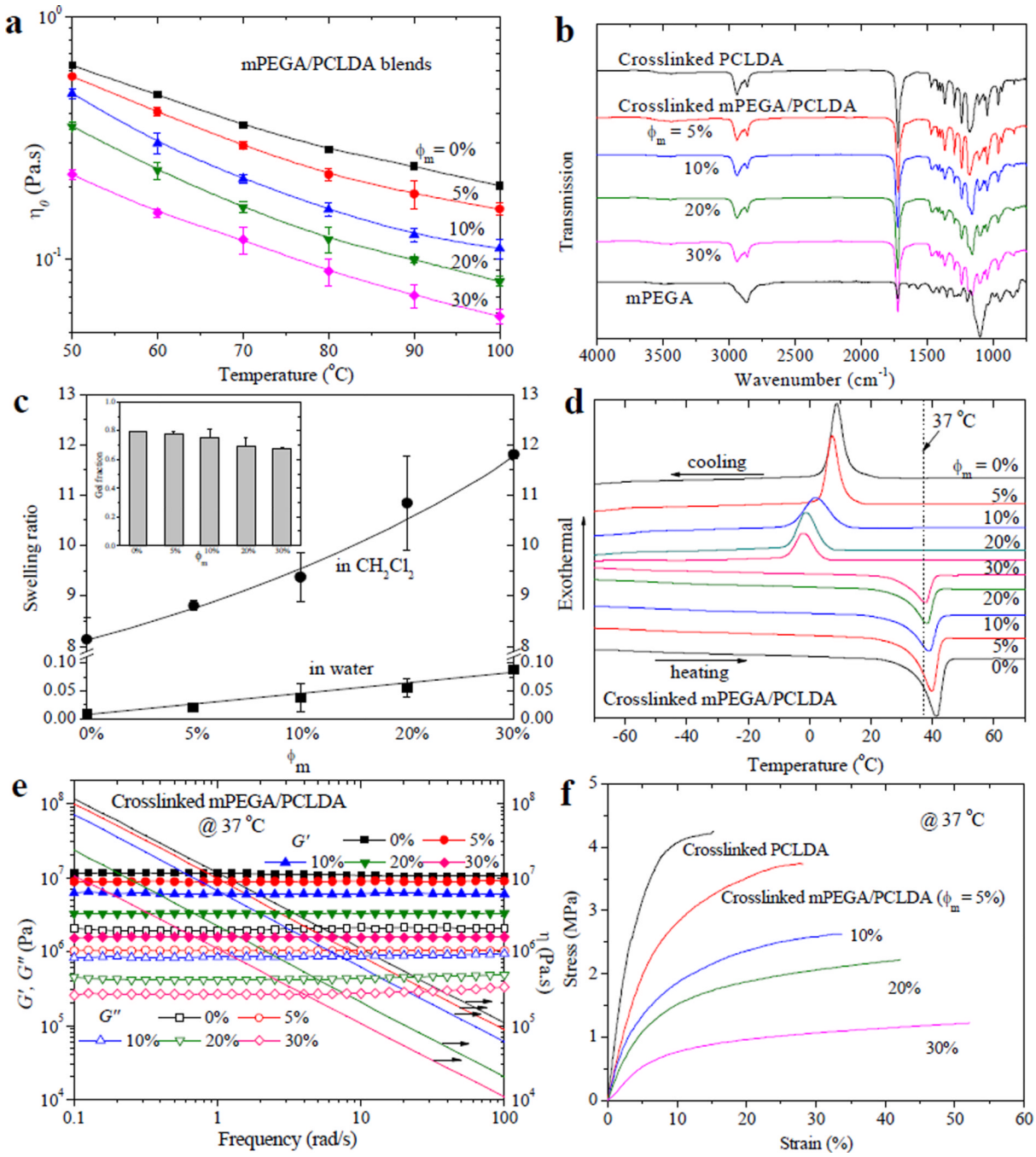

Figure 2.

Physical properties of uncrosslinked and crosslinked mPEGA/PCLDA samples. (a) Temperature dependence of zero-shear viscosity η_0 for uncrosslinked samples. (b) FTIR spectra of mPEGA and crosslinked samples. (c) Swelling ratios of crosslinked samples in CH_2Cl_2 and water. Inset: Gel fractions of crosslinked samples obtained in CH_2Cl_2. (d) DSC curves of crosslinked samples. (e) Storage modulus G' (solid symbols), loss modulus G'' (open symbols) and viscosity η (lines) vs. frequency for crosslinked samples at 37 °C. (f) Tensile stress-strain curves of crosslinked samples at 37 °C.

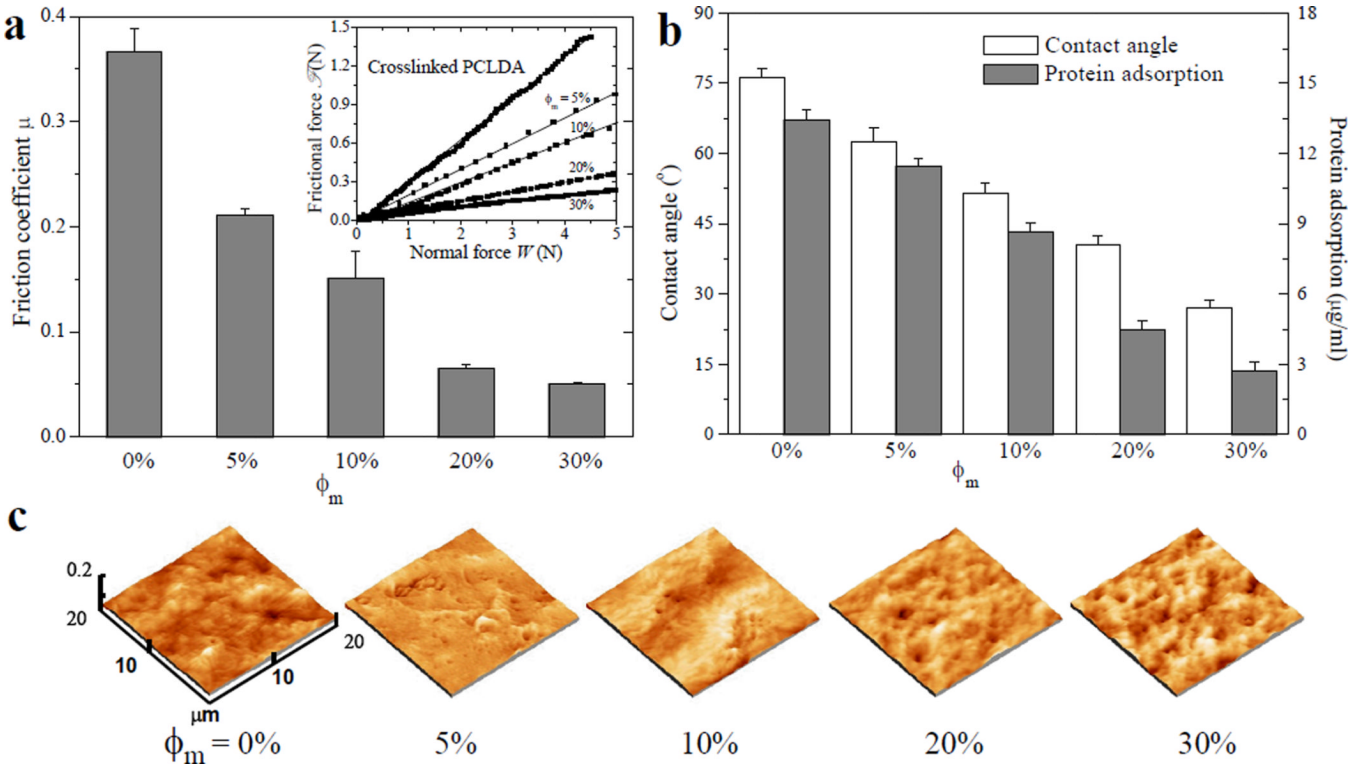

Figure 3.

Surface properties of crosslinked mPEGA/PCLDA disks. (a) Frictional coefficients between a stainless steel plate and hydrated polymer disks. Inset: Frictional force vs. normal force. (b) Water contact angle and protein adsorption. (c) AFM images. Significant difference ($p < 0.05$) is between any two groups in (a) and (b).

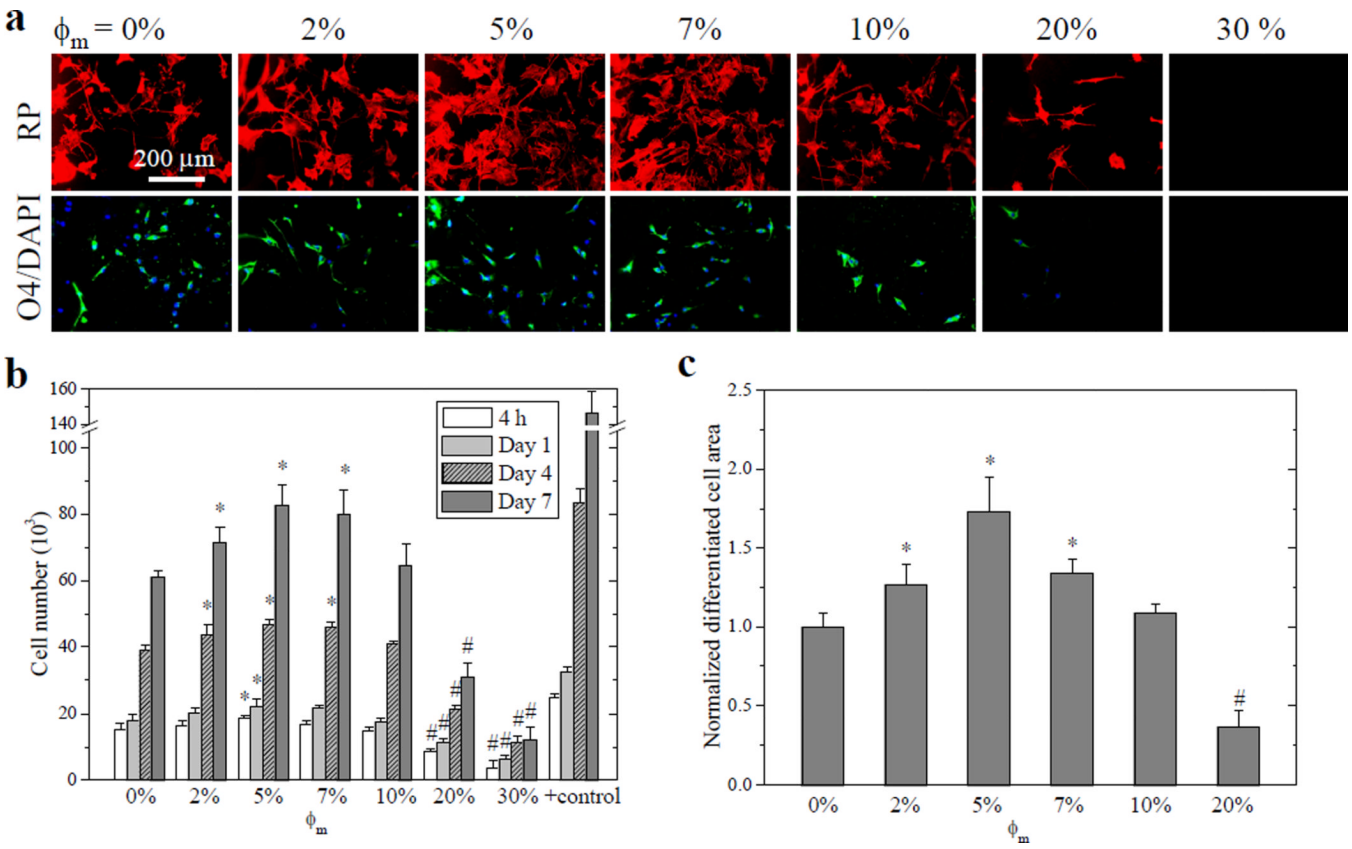

Figure 4.

Rat SpL201 cell attachment, proliferation, and differentiation on crosslinked mPEGA/PCLDA disks. (a) Fluorescent images of SpL201 cells stained using rhodamine-phalloidin (RP, red, top row), O4-positive areas (green, bottom row) and nuclei (blue) stained using 4', 6-diamidino-2-phenylindole (DAPI) of differentiated SpL201 cells upon forskolin treatment at day 7 post-seeding. Scale bar of 200 μm is applicable to all. (b) SpL201 proliferation at days 1, 4, and 7, compared with cell-seeded tissue culture polystyrene (TCPS) as positive control. (c) Normalized area positive to O4 antibody for SpL201 cells at day 7. *: significantly higher ($p < 0.05$); #: significantly lower ($p < 0.05$) than the corresponding data on crosslinked PCLDA disks.

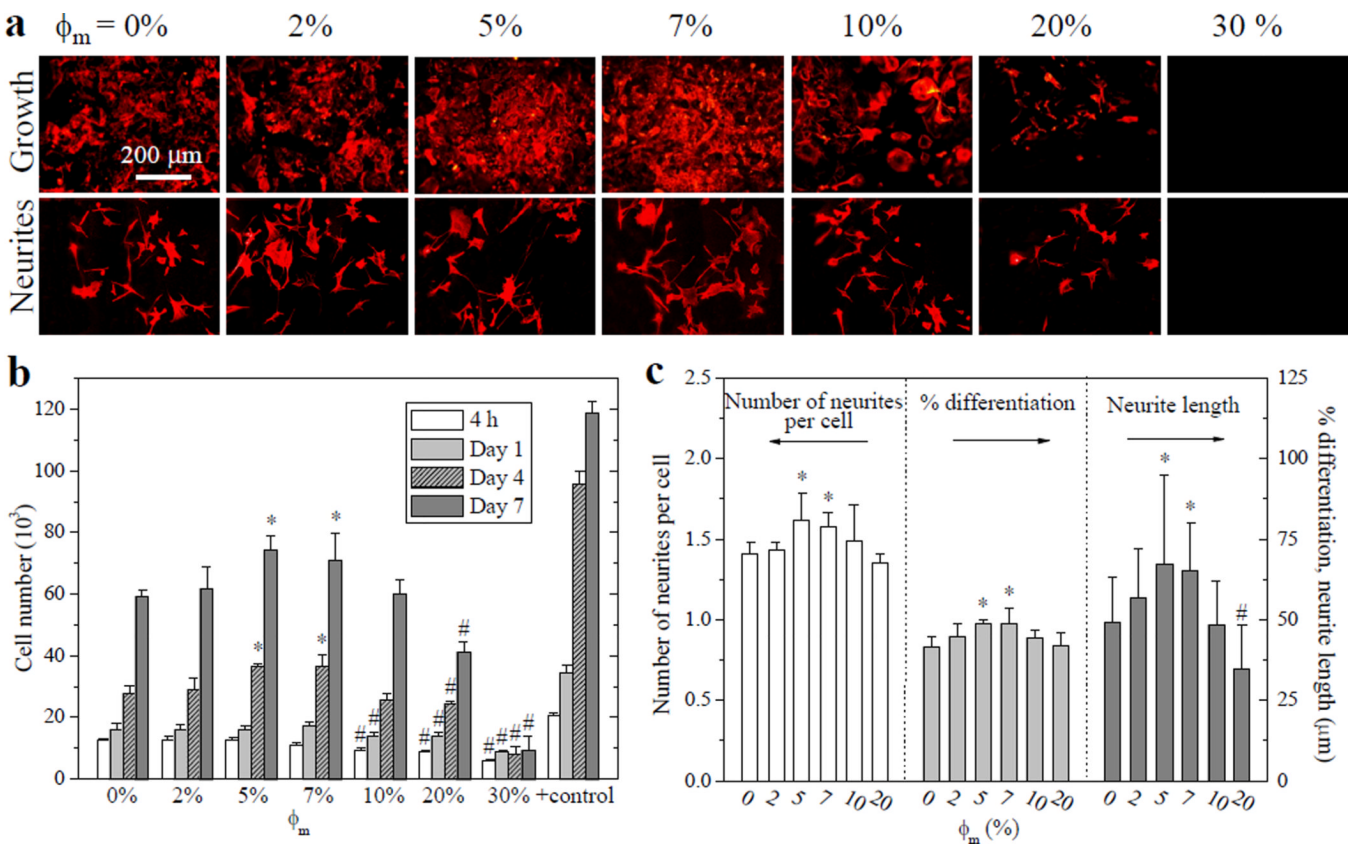

Figure 5.

Rat PC12 cell attachment, proliferation, and differentiation on crosslinked mPEGA/PCLDA disks. (a) Fluorescent images stained using RP for PC12 cell growth (top row) and NGF-induced neurites (bottom row) at day 7 post-seeding. Scale bar of 200 μm is applicable to all. (b) PC12 cell attachment at 4 h and proliferation at days 1, 4, and 7, compared with TCPS as positive control. (c) Quantification of PC12 neurites at day 7 using the number of neurites per cell, percentage of differentiated cells, and neurite lengths. *: significantly higher ($p < 0.05$); #: significantly lower ($p < 0.05$) than the corresponding data on crosslinked PCLDA disks.

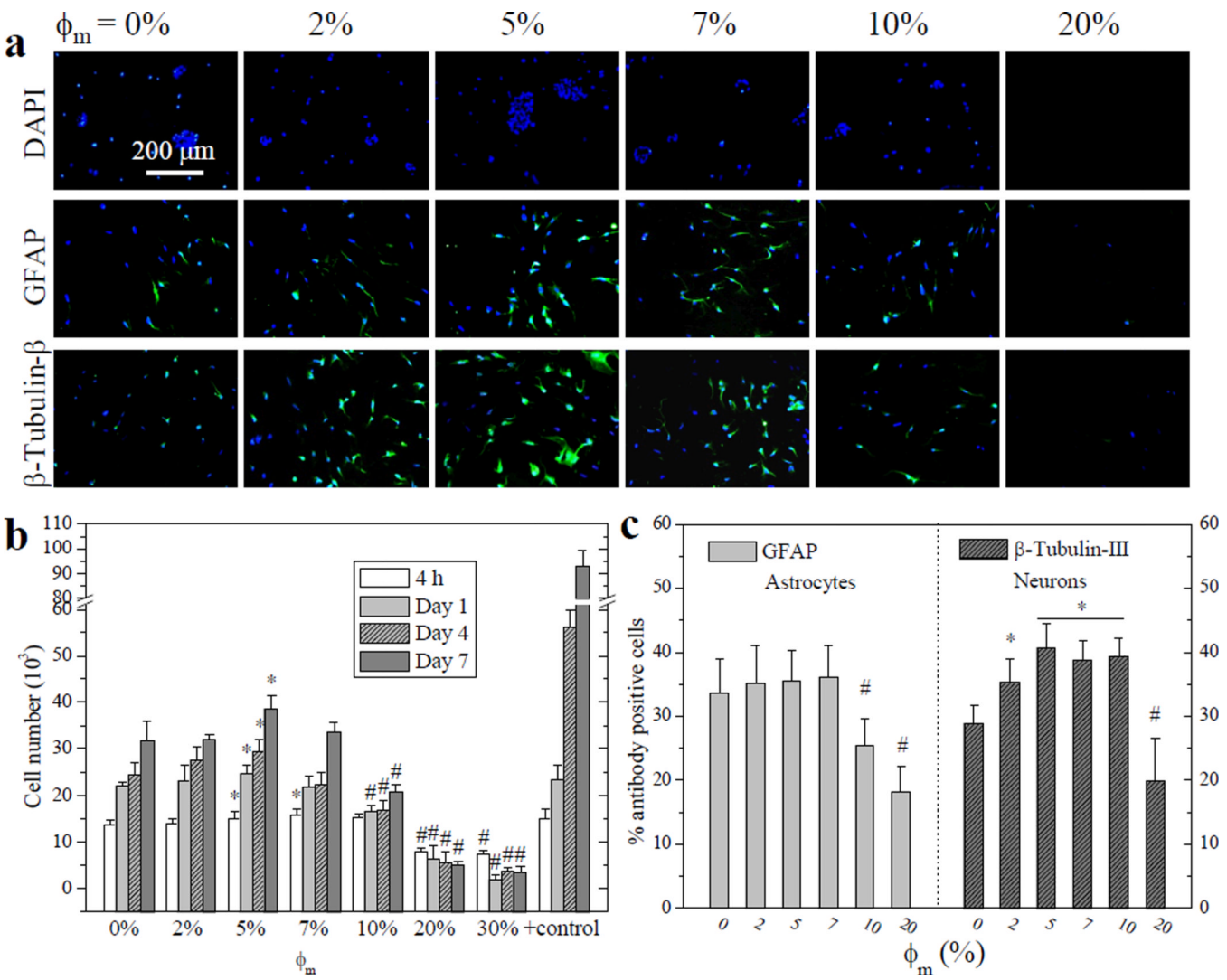

Figure 6.

E14 mouse NPC attachment, proliferation, and differentiated lineages on crosslinked mPEGA/PCLDA disks. (a) Fluorescent images of neurospheres stained using DAPI (blue, top row), differentiated astrocytes stained using anti-GFAP (green, middle row), and neurons stained using anti-β-tubulin-III (green, bottom row) at day 7 post-seeding. Scale bar of 200 μm is applicable to all. (b) NPC proliferation at days 1, 4, and 7, compared with TCPS as positive control. (c) Quantification of percentage of differentiated astrocytes and neurons at day 7. *: significantly higher ($p < 0.05$); #: significantly lower ($p < 0.05$) than the corresponding data on crosslinked PCLDA disks.

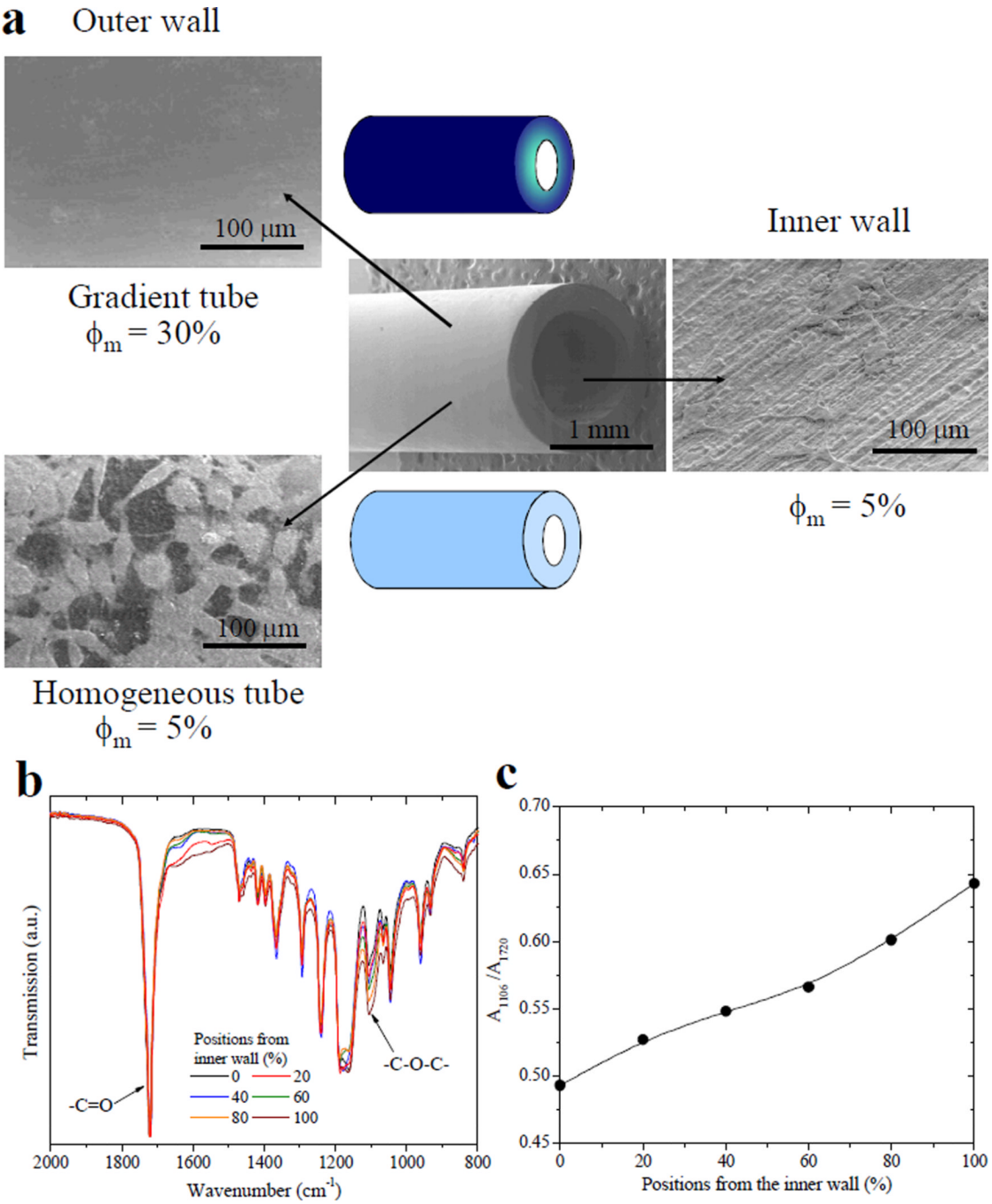

Figure 7.

Crosslinked mPEGA/PCLDA nerve tubes with two different structures. (a) SEM images of the tubes and SpL201 cells attached on the inner and outer walls of the tubes at day 1 post-seeding. For the homogeneous tube, ϕ_m is 5% everywhere. For the compositional-gradient tube, ϕ_m is 5% on the inner wall while it increased gradually to 30% on the outer wall. (b) FTIR spectra of the cross section of the gradient tube wall at different positions from the inner wall to the outer wall, represented by the percentage of the total wall thickness. (c) The ratios of the absorption at 1106 cm^{-1} (A_{1106}) for asymmetric C-O-C band to that at 1720 cm^{-1} (A_{1720}) for the C=O band for indicating the composition of PEG along the wall thickness.

Table 1

Thermal, mechanical and surface properties of crosslinked mPEGA/PCLDA

ϕ_m	T_g[°C]	T_c[°C]	ΔH_c [J g^{-1}] [a]	T_m [°C]	ΔH_m [J g^{-1}] [b]	χ_c [c]	G [MPa] [d]	E [MPa] [e]	σ_b [MPa] [f]	ε_b [%] [g]	R_{rms} [nm] [h]
0	−60.9	8.9	47.7	41.2	51.3	0.37	10.9 ± 0.4	83.0 ± 9.1	4.12 ± 0.44	15.9 ± 4.2	13.7 ± 2.8
5%	−59.4	7.4	43.9	39.7	47.7	0.36	8.9 ± 0.1	46.1 ± 7.2	3.66 ± 0.17	30.5 ± 6.9	17.9 ± 3.2
10%	−58.6	1.8	33.9	39.1	35.9	0.29	6.0 ± 0.3	32.0 ± 7.5	3.22 ± 0.52	36.9 ± 10.0	16.7 ± 2.7
20%	−57.9	−1.3	30.7	38.2	30.5	0.27	3.2 ± 0.2	17.8 ± 6.7	2.46 ± 0.58	40.0 ± 10.5	14.4 ± 4.9
30%	−57.4	−2.2	25.2	37.6	24.5	0.25	1.5 ± 0.2	8.9 ± 3.3	1.58 ± 0.36	46.1 ± 14.4	14.5 ± 4.8

[a] Heat of crystallization.

[b] Heat of fusion.

[c] Crystallinity calculated using the equation of $[\Delta H_m/(\phi_{PCL}\Delta H_m^C)/(1-\phi_m)] \times 100\%$, where ΔH_m^C of completely crystalline PCL is 135 J g^{-1} and ϕ_{PCL} is 96.9%.[6,11]

[d] Shear modulus measured at 37 °C.

[e] Tensile modulus,

[f] stress and

[g] strain at break measured at 37 °C.

[h] rms roughness calculated from AFM images.